SCIENCE CHINA
Life Sciences

• RESEARCH PAPERS •

October 2010 Vol.53 No.10: 1181–1188
doi: 10.1007/s11427-010-4069-2

# Structural characteristics of the hydrophobic patch of azurin and its interaction with p53: a site-directed spin labeling study

XU Chao[1,2], YIN JunJie[3] & ZHAO BaoLu[1,2*]

[1]*State Key Laboratory of Brain and Cognitive Science, Institute of Biophysics, Chinese Academy of Sciences, Beijing 100101, China;*
[2]*Graduate University of the Chinese Academy of Sciences, Beijing 100049, China;*
[3]*Center for Food Safety and Applied Nutrition, Food and Drug Administration, College Park, MD 20740, USA*

Received April 12, 2010; accepted May 25, 2010

Site-directed spin labeling (SDSL) is a powerful tool for monitoring protein structure, dynamics and conformational changes. In this study, the domain-specific properties of azurin and its interaction with p53 were studied using this technique. Mutations of six residues, that are located in the hydrophobic patch of azurin, were prepared and spin labeled. Spectra of the six azurin mutants in solution showed that spin labeled residues 45 and 63 are in a very restricted environment, residues 59 and 65 are in a spacious environment and have free movement, and residues 49 and 51 are located in a relatively closed pocket. Polarity experiments confirmed these results. The changes observed in the spectra of spin labeled azurin upon interaction with p53 indicate that the hydrophobic patch is involved in this interaction. Our results provide valuable insight into the topographic structure of the hydrophobic domain of azurin, as well as direct evidence of its interaction with p53 in solution via the hydrophobic patch. Cytotoxicity studies of azurin mutants showed that residues along the hydrophobic patch are important for its cytotoxicity.

**azurin, p53, spin label, protein-protein interaction, anticancer, ESR**

**Citation:** Xu C, Yin J J, Zhao B L, *et al*. Structural characteristics of the hydrophobic patch of azurin and its interaction with p53: a site-directed spin labeling study. Sci China Life Sci, 2010, 53: 1181−1188, doi: 10.1007/s11427-010-4069-2

It has been known for more than a century that some bacteria have the ability to kill cancer cells. Current research aims at identifying bacterial toxins to fight cancer [1]. Azurin is a copper-containing enzyme that acts as an electron transfer shuttle in *Pseudomonas aeruginosa* and other bacteria. Azurin is secreted into the growth medium and has been reported to promote cancer cell death *in vitro* [2–4].

The chemical structure of azurin has been extensively studied [5–7]. The protein consists of a two β-sheet-sandwich with eight β-stands arranged in a Greek-key topology. *In vivo*, a redox active copper is coordinated to the protein allowing for electron-transfer activity. The copper in azurin can be removed, creating apo-azurin, or exchanged for other metals, without any change in the overall structure [8]. The presence of a disulfide linkage makes azurin fairly resistant to thermal denaturation [9,10]. Azurin possesses a relatively large hydrophobic patch. The hydrophobic patch is important for its interaction with p53 and also plays an important role in the internalization of azurin in cancer cells, partly by a receptor-mediated endocytic process [11–13].

Understanding the structure of the hydrophobic patch in azurin, both the crystal structure and its structure in solution, is crucial for delineating the mechanism of its anticancer activity.

The transcription factor p53 is responsible for maintaining the integrity of the genome [14–17]. p53 is generally

*Corresponding author (email: zhaobl@sun5.ibp.ac.cn)

present at a low level in mammalian cells because of its short half-life of a few minutes. This short half life is primarily due to its degradation through the ubiquitin proteasome pathway. Azurin may form a complex with p53, thereby stabilizing p53 [18–21]. Stabilization of p53 leads to increases in its intracellular level, which in turn stimulates its apoptosis-promoting activity by regulating expression of pro-apoptotic proteins such as Bax [3,4]. Some *in vitro* studies have revealed that there is a direct interaction between azurin and p53. The hydrophobic patch has been proposed to be involved in complex formation with p53 [19,20], but there is no direct evidence to confirm this hypothesis.

Recent studies in this field have made use of site-directed spin labeling (SDSL), a powerful tool for monitoring changes in the structure and dynamics of proteins in solution [22,23]. In SDSL, a nitroxide side chain is introduced via a mutagenic cysteine substitution followed by modification of the sulfhydryl group with a specific nitroxide reagent. The rotation of the spin labeled nitroxide influences the line shape of the ESR spectrum. Therefore, the ESR spectrum of a spin label provides valuable information about its structural environment [24–26]. Spin labels serve as excellent probes of the solvent accessibility, local geometry and flexibility of proteins, as well as protein structural changes induced by their interactions with other proteins or with their environment.

In this study, SDSL was used to investigate the structural characteristics of the hydrophobic patch of azurin and its interaction with p53. Six residues of the hydrophobic patch of azurin were individually replaced by cysteines and spin labeled. The resulting ESR spectra provide a detailed insight into the topographic structure of the hydrophobic domain of azurin and its interaction with p53.

## 1 Materials and methods

### 1.1 Materials

All the enzymes used in preparing mutations were obtained from Fermantas. 5,5′-Dithio-bis(2-nitrobenzoic acid) (DTNB) was obtained from Sigma Chemical Co. (St. Louis, MO). Dulbecco's modified Eagle's medium (DMEM) and fetal calf serum (FCS) were obtained from Gibco. 4-(2-hydroxyethyl)-1-piperazineethanesulfonic acid (HEPES), isopropyl beta-D-thiogalactopyranoside (IPTG) and 3-(4,5-dimethylthiazol-2-yl)-2,5-diphenyl-tetrazolium-bromide (MTT) were purchased from Amresco. BCA Protein Assay kits were purchased from Pierce. The spin label reagent (1-oxyl-2,2,5,5-tetrame-thylpyrroline-3-methyl)-methanethiosulfonate was from the Toronto Research Chemicals Incorporation. J774 cells were provided by the Cell Resource Center, Chinese Academy of Medical Sciences/Peking Union Medical College (CAMS/PUMC). All other chemicals were made in China and were of analytical grade.

### 1.2 Mutagenesis and protein purification

Site-directed mutagenesis of the azurin gene was performed using a QuikChange Site-directed Mutagenesis Kit (Stratagene) in accordance with the manufacturer's instructions. A base azurin mutant, M(C112S), was first constructed by substituting the cysteine at residue 112 for serine. Six double mutants (C112S/G45C, C112S/V49C, C112S/S51C, C112S/V59C, C112S/G63C and C112S/A65C), in which one of the hydrophobic patch residues was substituted with cysteine, were then constructed using M(C112S) as a starting point. For example, the residue Gly45 in M(C112S) was substituted by cysteine to obtain the double mutant C112S/G45C. Mutations were confirmed by DNA sequencing.

Azurin was purified from recombinant *E. coli* cells in accordance with a previously published method [27]. The protein was expressed in BL21(DE3) cells, which were grown at 37°C to an $A_{600} \approx 0.8$ before induction with 0.5 mmol $L^{-1}$ IPTG and culturing overnight at 25°C. The cells were harvested by centrifugation and sonicated in 50 mmol $L^{-1}$ NaCl and 50 mmol $L^{-1}$ Tris-HCl (pH 8.0). The soluble lysate was loaded onto a Ni-Sepharose affinity column and eluted with an imidazole gradient (0–500 mmol $L^{-1}$). The eluent was collected and subjected to electrophoresis and the protein concentration of azurin was determined using a BCA kit.

Further purification was achieved using SP-Sepharose cation exchange chromatography. Fractions containing azurin were pooled and dialyzed against PBS. A vector containing the full-length p53 was a kind gift from Professor Bi LiJun. p53 was purified in accordance with a previously published method [28]. A further purification step, using affinity chromatography with heparin-Sepharose and a NaCl gradient (0–1 mol $L^{-1}$) for elution, was added.

### 1.3 Quantitative determination of the sulfhydryl groups in azurin and its mutants

DTNB (or Ellman's reagent) has been used extensively to quantitatively determine the sulfhydryl concentration. The sulfhydryl concentration was determined in accordance with a previously published method [29]. The absorbance of 6.7 μmol $L^{-1}$ azurin or its mutants in 100 μmol $L^{-1}$ DTNB, 100 mmol $L^{-1}$ Tris-HCL (pH 8.0) was measured at 412 nm using a UV-Vis spectrophotometer (Hitachi, Tokyo, Japan).

### 1.4 J774 cell culture and cytotoxicity assay

J774 cells were cultured in DMEM medium supplemented with 10% fetal bovine serum, at 37°C in a humidified incubator with 5% $CO_2$. The cytotoxicity of azurin was meas-

ured with the MTT assay, conducted in accordance with a previously published method [2,3] with some modifications. About $5\times10^4$ cells per well were seeded onto 96-well culture plates in 120 μL of DMEM medium. After overnight culturing, the medium was replaced with fresh medium containing different concentrations of azurin. The culture medium was replaced after 24 h with fresh medium free of serum, containing 0.5 mg $mL^{-1}$ MTT solution. After incubation for 3 h at 37°C, the formation was dissolved in DMSO and its absorbance read at 595 nm.

### 1.5 Spin labeling and ESR measurements

The reaction of the spin label methanethiosulfonate with cysteine produced a new side-chain containing a disulfide-linked nitroxide, which will be referred to here as R1 (Figure 1A). G45R1 denotes a mutant in which the native glycine at residue 45 was replaced by the spin labeled amino acid R1. The reaction mixture, containing a 10:1 spin label: azurin (30 μmol $L^{-1}$) molar ratio in 1 mL PBS was incubated overnight [30,31]. Excess spin label was removed by dialyzing against PBS. Labeled proteins were then concentrated to 150 μmol $L^{-1}$ using filtration units (Millipore 3000 MW cutoff). 30-μL samples were loaded into micro-capillary tubes, and ESR spectroscopy was performed on an X-band spectrometer (Bruker ER-200D-SRC). All spectra were recorded at 20°C. The incident microwave power was 20 MW and the modulation amplitude was 1.0 Gauss. Signal-averaged spectra (3 scans) were obtained with a 150 Gauss sweep.

The six azurin patch double mutants were spin labeled separately (Figure 1B). The cysteines in mutant C112S/V49C and C112S/S51C could only be labeled in a denaturing environment of 2 mol $L^{-1}$ urea, probably because they are located in the interior of the hydrophobic patch and therefore inaccessible to the spin label reagent. The spectra of these two mutants were measured after thorough dialysis against PBS to remove the urea. Other azurin mutants were readily spin labeled in PBS buffer. The rotational correlation time, $\tau_c$, or the ratio of the strong immobility component to the weak immobility component (S/W) were calculated using the spectral parameters from the reference [32].

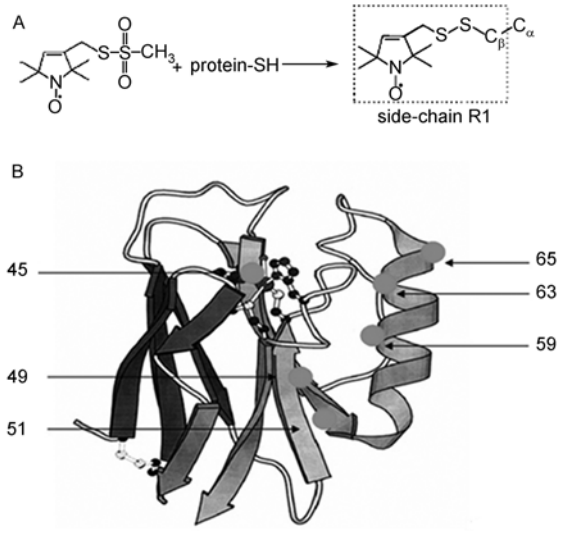


**Figure 1** A, Spin labeling reaction. Reaction of methanethiosulfonate with cysteine to produce the nitroxide side chain R1 [22]. B, Spin labeled sites in azurin. Six residues along the hydrophobic patch were replaced separately by cysteines and spin labeled. This figure of azurin was taken from [35].

ESR broadening was induced by the paramagnetic reagent $NiCl_2$ [33,34]. Changes in the spectra before and after adding $NiCl_2$ (150 μmol $L^{-1}$) to the solution of labeled protein (150 μmol $L^{-1}$) were measured. Finally, the structural changes of azurin during its interaction with p53 were studied. The six azurin double mutants (150 μmol $L^{-1}$) were mixed separately with p53 (35 μmol $L^{-1}$), at a molar ratio of 4∶1 azurin∶p53 (in accordance with Apiyo and Wittung [20]). ESR spectra of azurin free in solution and in complex with p53 were compared.

### 1.6 Statistical analysis

One-way ANOVA was used to estimate the overall significance followed by post hoc Tukey's tests corrected for multiple comparisons [36]. Data are presented as mean±SEM. A probability level of 5% ($P$<0.05) was considered significant.

## 2 Results

### 2.1 Mutagenesis and protein purification

To study the structural characteristics of the hydrophobic patch of azurin and its interaction with p53, six double mutants, namely C112S/G45C, C112S/V49C, C112S/S51C, C112S/V59C, C112S/G63C and C112S/A65C were prepared. Mutations were confirmed by DNA sequencing and the single free sulfhydryl groups introduced into the mutants were examined using Ellman's Test. Azurin and its mutants were purified using a Ni affinity column and cation exchange chromatography. The wild type azurin, mutant M (C112S) and six double mutants appeared as a single band of 15 kD on a 15% SDS-PAGE, while purified full length p53 appeared as a 53 kD band (Figure 2).

### 2.2 Quantitative determination of the sulfhydryl in azurin and its mutants

There are three cysteine residues in azurin. Cysteine 3 and cysteine 26 form a disulfide linkage, whereas cysteine 112 is free [9]. The sulfhydryl content was determined using the Ellman's test [29]. Wild type azurin was found to have only one sulfhydryl, whereas there was no sulfhydryl in M(C112S).

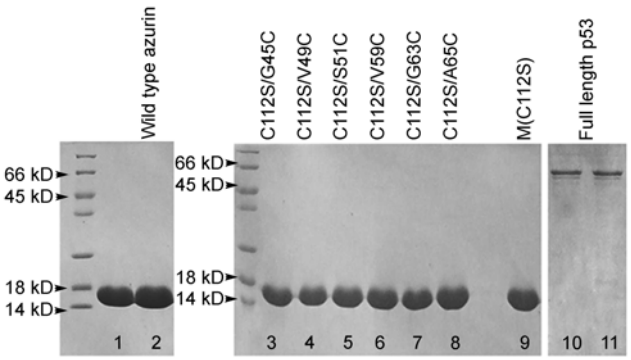


**Figure 2** SDS-PAGE of the purified proteins. Hyper-expressed azurin and its mutants in *E. coli* were purified by Ni-affinity and SP-Sepharose columns. Wild type azurin (lanes 1 and 2), six double mutants (lanes 3–8: C112S/G45C, C112S/V49C, C112S/S51C, C112S/V59C, C112S/G63C and C112S/A65C), mutant M(C112S) (lane 9), and purified full length p53 (lanes 10 and 11) are shown.

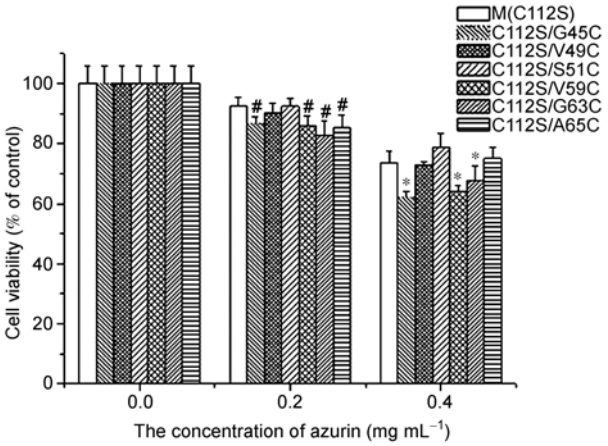


**Figure 3** Cell viability of J774 cells treated with azurin mutants. J774 cells were treated with various concentrations of azurin mutants for 24 h and cell viability was measured with the MTT assay. Each data point is the mean of six independent trials. * (0.2 mg mL$^{-1}$) and # (0.4 mg mL$^{-1}$) vs. M(C112S) ($P$<0.05).

This result is in accordance with the crystal model (Figure 1B), and suggests that the azurin protein expressed in *E. coli* folded and formed the disulfide bond properly. The free sulfhydryl content was then determined in the six double mutants of azurin, each of which contained one sulfhydryl group.

### 2.3 Cytotoxicity of azurin towards J774 cells

To ascertain whether mutagenesis of the hydrophobic patch influenced the cytotoxicity of azurin towards cancer cells, the cytotoxicity of azurin and its mutants toward J774 macrophage cells was examined. Mutant M(C112S) had similar cytotoxicity as apo-azurin and lower cytotoxicity than holo-azurin (data not shown), in agreement with the results reported by Goto *et al.* [18].

Our results indicate that secondary mutagenesis at residues 45, 59 or 63 slightly increased the cytotoxicity of azurin compared with mutant M(C112S) ($P$<0.05) (Figure 3). The double mutants, C112S/V49C, C112S/S51C and C112S/A65C, were observed to have similar cytotoxicity values to the value measured for M(C112S).

### 2.4 Topography around the hydrophobic patch of azurin

As described above, cysteine 112 in wild type azurin was first replaced by a serine and then a single cysteine was introduced to replace one of the residues along the hydrophobic patch of azurin, creating a series of six mutants which were then spin labeled. The ESR spectra of spin labeled cysteines in the patch (Figure 4, left traces) provide information about the dynamic structure of azurin in solution. The spectra of the six residues can be divided into three groups according to the environment and movement of the nitroxide.

G45R1 and G63R1 form a group with a notably strong immobility component in the spectra. The movements of the nitroxide at the two sites are restricted by the environment of the labeled site. We calculated the ratio of the strong immobility component to the weak immobility component (S/W) to evaluate the movement of the two sites. G63R1 (S/W=0.529±0.014) was more restricted than G45R1 (S/W=0.397±0.013).

By contrast, residue A65R1 ($\tau_c$=(1.67±0.15)×10$^{-9}$ s) is on the surface and its ESR spectrum was the most mobile of the spin labeled residues. Residue V59R1 is located in the hydrophobic patch, but its mobility was found to be fairly free ($\tau_c$=(1.94±0.07)×10$^{-9}$ s). These two residues constitute a second group, which can be spin labeled directly and has a high mobility.

Residues C49 and C51, forming the third group, could only be labeled in a denatured environment. After dialyzing against PBS, the refolded mutants should have resumed their native structure and function (explained in the discussion). When the spectra of the refolded mutants were recorded, the movements of nitroxide in V49R1 and S51R1 were more mobile (49R1, $\tau_c$=(3.45±0.10)×10$^{-9}$ s; 51R1, $\tau_c$=(4.76±0.27)×10$^{-9}$ s) than those of group one, suggesting that residues 49 and 51 are located in a relatively spacious and closed environment.

### 2.5 Polarity around the hydrophobic patch of azurin

The polarity surrounding the nitroxide groups is related to their aqueous or hydrophobic properties, and can be determined by the broadening of the ESR spectrum using paramagnetic reagents. The degree of ESR broadening reflects local polarity and the accessibility of the nitroxide to the polar reagent. Increased broadening obtained with polar paramagnetic reagents such as $NiCl_2$ (used in this study) reflects stronger local polarity. The level of reduction in the

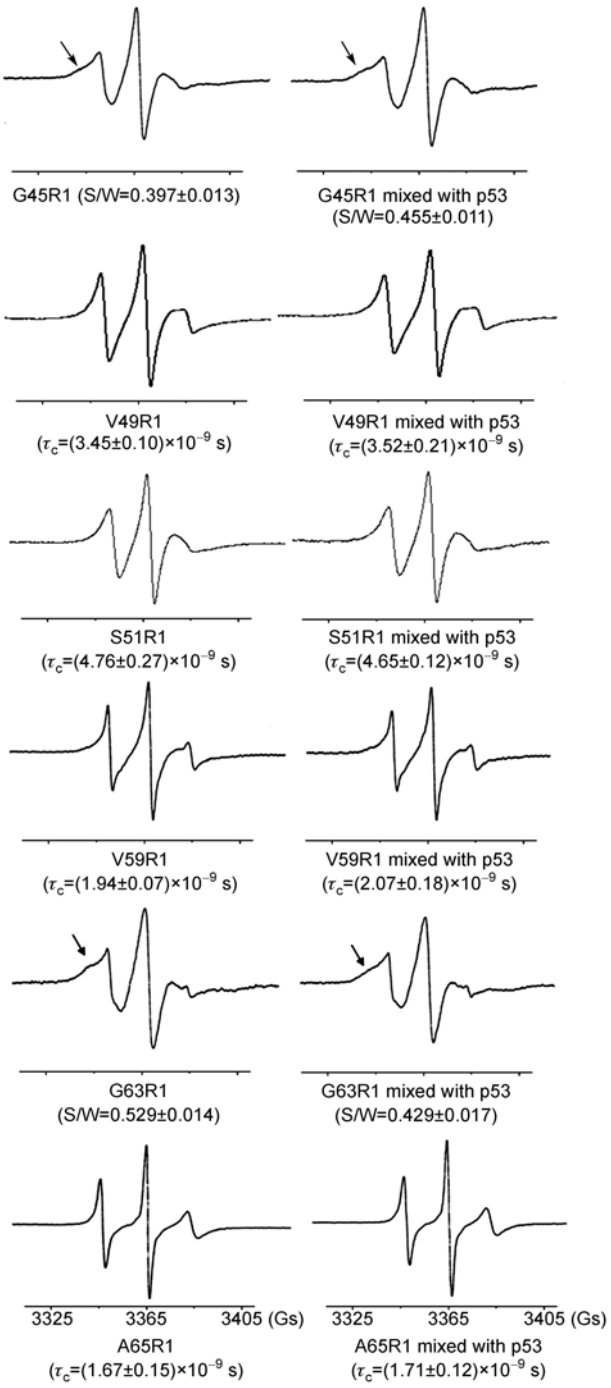


**Figure 4** Effect of the interaction between azurin and p53 in solution on spin labeling spectra. Traces on the left-hand side are spectra of spin labeled azurin mutants alone, and those on the right-hand side are spectra of azurin mutants mixed with p53. There were significant changes in the spectra of G45R1 and G63R1 (indicated by arrows, $P$<0.05) during the interaction (expressed by the ratio of the strong immobility component to the weak immobility component S/W). There were no significant changes in the spectra of the other labeled sites (expressed by $\tau_c$).

signal amplitude represents the level of ESR broadening.

G63R1 and A65R1 showed greater broadening (54.3%±3.6% and 47.2%±2.9%, respectively) (Figure 5), indicating

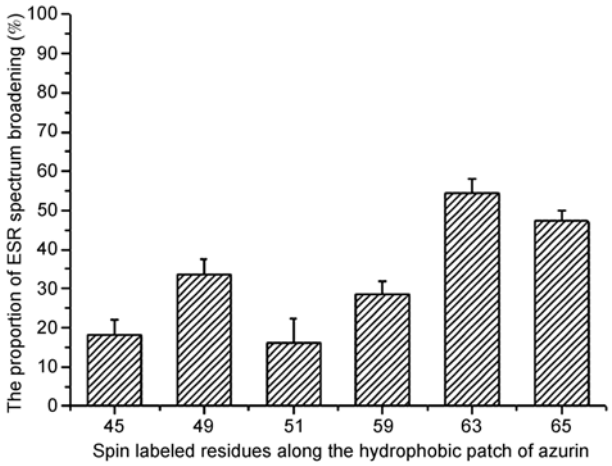


**Figure 5** Broadening of the ESR spectra of the spin labeled mutants of azurin with paramagnetic $NiCl_2$ was proportional to the reduction in signal amplitude. The reduction in the amplitude of ESR spectra was measured after adding paramagnetic $NiCl_2$. Each value is the mean of three independent trials and is expressed as the percentage of the amplitude of the equivalent spectrum without $NiCl_2$. The values represent the different levels of ESR broadening in different mutants.

that the two labeled nitroxides are more accessible to the polar reagent $NiCl_2$, whereas the other four spin labeled residues showed less broadening (G45R (18.3%±3.9%), V49R1 (33.7%±3.9%), S51R1 (16.2%±6.0%) and V59R1 (28.6%±3.2%)).

### 2.6 Changes in ESR spectra induced by interactions with p53

ESR line shape changes (Figure 4) reflect structural changes involving different residues upon interacting with p53. The increase in S/W from 0.397±0.013 to 0.455±0.011 indicates a decrease in mobility at residue 45. By contrast, a decrease in S/W from 0.529±0.014 to 0.429±0.017 indicates a change from immobility to mobility at residue 63. Both sites are located around the opening of the hydrophobic patch. Changes in the spectra reflect the tertiary contact and backbone dynamics of the spin labeled residues.

The mobility of other sites is expressed as $\tau_c$. There were no significant changes in the spectra of residues V49R1, S51R1 and V59R1, which are located deep in the interior of the hydrophobic patch. The spectrum of residue A65R1, which is located on the surface of azurin, also showed no significant changes. The absence of statistically significant changes in $\tau_c$ indicates that these residues are not directly involved in the interaction with p53.

## 3 Discussion

Some studies on molecular interactions between azurin and p53 have been conducted. Formation of the complex was characterized using glycerol-gradient ultracentrifugation

and GST pull-down experiments [18,19]. In addition, Cannistraro *et al.* [37] investigated this interaction using single-molecule force spectroscopy, and also proposed a docking model of the interaction based on computational methods [38]. The interaction of azurin with p53 has been suggested to involve a hydrophobic patch on azurin [19,20], which is normally involved in interactions with other redox partners. However, there remains no direct experimental evidence describing the mechanism of this protein-protein interaction and the possible role of this hydrophobic patch in complex formation.

Site-directed spin labeling (SDSL) has proven to be a powerful tool in following the structural and dynamic changes of proteins in solution. Here we used this method to study the topographical structure around the hydrophobic patch and the interaction of azurin with p53. In SDSL, a single free cysteine is introduced at a specific position and spin labeled. In wild type azurin, C112 is one of the ligands in the copper active site, but its presence interferes with the spin labeling procedure. Because copper is not essential for the cytotoxicity of azurin [18], the C112 residue of wild type azurin was substituted, to form a "base" mutant M(C112S). Spin labeling of the base mutant M(C112S) gave no ESR signal, as there was no free sulfhydryl to be labeled in M(C112S). A single cysteine was then introduced into the patch. Amino acids which had similar properties to cysteine were chosen for substitution.

The ESR spectra obtained reflect side-chain motions and local topography. Residues G45R1 and G63R1 (Figure 4, left traces) form a group in which there is an obvious strong immobility component in the spectra, indicating that the movements of the nitroxide at the two sites are highly restricted by the surrounding residues. A second group, consisting of residues V59R1 and A65R1, had a high mobility. From the crystal model (Figure 1B), we can see that residue V59R1 seems to be located deeper in the interior of the hydrophobic patch compared with G45R1 and G63R1, while its mobility is fairly free ($\tau_c$=(1.94±0.07)×$10^{-9}$ s). This effect may be due to local environmental differences. We speculate that G45R1 and G63R1 are situated around the opening of the hydrophobic patch and that the density of neighboring residues around the nitroxide is higher. By contrast, V59R1 lies in a relatively spacious environment in the hydrophobic patch

In the third group, the cysteines in C112S/V49C and C112S/S51C are highly inaccessible to the spin label reagent and could only be spin labeled following partial denaturation. The accessibility of the cysteines to the spin label reagent was different to that of the Ellman's reagent, which could react directly with the sulfhydryls in the mutants. It is possible that differences in hydrophobicity are responsible for the differences in these reactions. The ESR spectra of spin labeled C112S/V49C and C112S/S51C were measured after dialysis. Refolded mutants had similar cytotoxicity values as the untreated purified mutants (data not shown), suggesting that the refolded mutants were able to resume their native structures and function properly after dialysis. From the ESR spectra (Figure 4, left traces), the residues V49R1 and S51R1 showed greater mobility (49R1, $\tau_c$=(3.45±0.10)×$10^{-9}$ s; 51R1, $\tau_c$=(4.76±0.27)×$10^{-9}$ s), compared with the spin labeled residues of the first group, indicating that residues 49 and 51 were located in a pocket that is buried in the interior of the hydrophobic patch. The results of the spin labeling are in accordance with the crystal structure of azurin, which shows that both V49R1 and S51R1 are located deep within the hydrophobic patch [5,6].

Solvent polarity along the hydrophobic patch was determined by examining ESR spectral broadening with paramagnetic $NiCl_2$. Accessibility to $NiCl_2$ reflects solvent polarity around the spin labeled nitroxides [33,34]. Four residues in the patch, G45R1, V49R1, S51R1 and V59R1 (Figure 5), have low accessibility to the polar $NiCl_2$, indicating that these four residues are located in the interior of azurin and are inaccessible to the polar reagent. By contrast, G63R1 and A65R1 have greater accessibility to $NiCl_2$, suggesting that G63R1 and A65R1 are in a more polar environment. Although the spectrum of G63R1 has an obvious strong immobility component and the movement of G63R1 is restricted, the polar agent was still able to reach this spin label.

ESR line shapes of the spin labeling spectra give information about structural changes, and the changes in structure reflect the dynamics underlying the function [22,23,31]. The changes in the ESR spectra are due to the contact between the labeled residues and p53. When bovine serum albumin was mixed with the labeled azurin, no changes in the spectra were observed, indicating that the changes in the concentration of the protein, which create a crowded environment to some extent, did not induce changes in the spectra. Only upon interaction of azurin with p53 did the spectra of azurin change. Comparative analysis of the spectra of the spin labeled mutants in solution and in complex with p53 allows us to detect structural changes in the hydrophobic patch upon formation of the p53-azurin complex.

Upon interacting with p53, the ESR spectra of G45R1 and G63R1 changed significantly (Figure 4). The S/W ratio increased significantly in G45R1, suggesting that p53 interacted with azurin around this site. Crowding at G45R1 induced a reduction in the mobility of the nitroxide label. By contrast, the S/W of G63R1 decreased upon interaction of p53 with azurin, indicating a reduction in tertiary interactions induced by the movement of the backbone around this site. We speculate that the helix in which G63R1 is located, rotates during the interaction, such that G63R1 is exposed near the surface of azurin where this residue has a greater mobility. It seems that a hydrophobic core, around G45R1 and away from G63R1, is formed for p53 docking. The docking induces changes in backbone dynamics around the two sites.

The mobility of nitroxide at the other sites was deter-

mined by $\tau_c$ (Figure 4). There were no significant changes in $\tau_c$ for V49R1, S51R1 and V59R1, which are located deep in the hydrophobic patch. This indicates that the residues around the opening of the patch, but not those in the interior of the patch, are involved in the interaction. The mobility of the nitroxide at A65R1 did not change significantly upon interaction with p53, indicating that the hydrophobic core formed for docking p53 is located distal from residue A65R1.

All six double mutants constructed based on M(C112S) had marked cytotoxicity towards J774 cancer cells, indicating that the introduction of cysteines in spin labeling did not disrupt the structure and function. It is interesting to note that secondary mutagenesis at residues 45, 59 and 63 slightly increased the cytotoxicity of azurin, indicating that these amino acids in the hydrophobic patch are important for determining the cytotoxicity of azurin. It should be noted that residues 45 and 63 are located around the opening of the hydrophobic patch, not deep within the patch. This result is in accordance with ESR spectra from the spin labeling experiment, which showed that G45R1 and G63R1 changed significantly during the interaction of azurin with p53. Further experiments are underway to examine whether the enhanced cytotoxicity of azurin after mutagenesis of residues 45, 59 and 63 is due to an increase in the stabilization of p53 upon binding with azurin, which in turn results in an enhancement of the intracellular levels of p53.

In conclusion, using SDSL we have described the topographic structure around the hydrophobic patch of azurin in solution and provide direct evidence that azurin interacts with p53 via its hydrophobic patch. Studies of the cytotoxicity of azurin mutants towards J774 cancer cells indicated that the amino acids of the hydrophobic patch are important for their cytotoxicity.

*We thank Professors Gao Jin and Bi LiJun for their kind gifts of plasmids for azurin and p53 expression, and Chen YongSheng for technical support with the ESR measurements. This work was supported by the National Natural Science Foundation of China* (*Grant No. 30370361*)*, the National Basic Research Program of China* (*Grant No. 2006CB500700*)*, and was partially supported by the Key Laboratory of Mental Health, Chinese Academy of Sciences.*

1 Fialho A M, Stevens F J, Das Gupta T K, *et al.* Beyond host-pathogen interactions: microbial defense strategy in the host environment. Curr Opin Biotechnol, 2007, 18: 279–286
2 Yamada T, Goto M, Punj V, *et al.* The bacterial redox protein azurin induces apoptosis in J774 macrophages through complex formation and stabilization of the tumor suppressor protein p53. Infect Immun, 2002, 70: 7054–7062
3 Yamada T, Goto M, Punj V, *et al.* Bacterial redox protein azurin, tumor suppressor protein p53, and regression of cancer. Proc Natl Acad Sci USA, 2002, 99: 14098–14103
4 Punj V, Bhattacharyya S, Saint-Dic D, *et al.* Bacterial cupredoxin azurin as an inducer of apoptosis and regression in human breast cancer. Oncogene, 2004, 23: 2367–2378
5 Nar H, Messerschmidt A, Van de Kampa R H, *et al.* Crystal structure of Pseudomonas aeruginosa apo-azurin at 1.85 Å resolution. FEBS Lett, 1992, 306: 119–124
6 Nar H, Messerschmidt A, Van de Kamp R H, *et al.* Crystal structure analysis of oxidized Pseudomonas aeruginosa azurin at pH 5.5 and pH 9.0. J Mol Biol, 1991, 221: 765–772
7 Adman E T, Stenkamp R E, Sieker L C, *et al.* A crystallographic model for azurin at 3 Å resolution. J Mol Biol, 1978, 123: 35–47
8 Nar H, Huber R, Messerschmidt A, *et al.* Characterization and crystal structure of zinc azurin, a by-product of heterologous expression in *Escherichia coli* of *Pseudomonas aeruginosa* copper azurin. Eur J Biochem, 1992, 205: 1123–1129
9 Bonander N, Karlsson BG, Vanngard T. Disruption of the disulfide bridge in azurin from Pseudomonas aeruginosa. Biochim Biophys Acta, 1995, 1251: 48–54
10 Milardi D, Grasso D M, Verbeet M Ph, *et al.* Thermodynamic analysis of the contributions of the copper ion and the disulfide bridge to azurin stability: synergism among multiple depletions. Arch Biochem Biophys, 2003, 414: 121–127
11 Van P G, Cigna G, Rolli G, *et al.* Electron-transfer properties of Pseudomonas aeruginosa Lys44, Glu64 azurin. Eur J Biochem, 1997, 247: 322–331
12 Yamada T, Fialho A M, Punj V, *et al.* Internalization of bacterial redox protein azurin in mammalian cells: entry domain and specificity. Cell Microbiol, 2005, 7: 1418–1431
13 Taylor B N, Mehta R R, Yamada T, *et al.* Noncationic peptides obtained from azurin preferentially enter cancer cells. Cancer Res, 2009, 69: 537–46
14 Yee K S, Vousden K H. Complicating the complexity of p53. Carcinogenesis, 2005, 26: 1317–1322
15 Vousden K H, Lu X. Live or let die: the cell's response to p53. Nat Rev Cancer, 2002, 2: 594–604
16 Ryan K M, Phillips A C, Vousden K H. Regulation and function of the p53 tumor suppressor protein. Curr Opin Cell Biol, 2001, 13: 332–337
17 Hofseth L J, Hussain S P, Harris C C. p53: 25 years after its discovery. Trends Pharmacol Sci, 2004, 25: 177–181
18 Goto M, Yamada T, Kimbara K, *et al.* Induction of apoptosis in macrophages by Pseudomonas aeruginosa azurin: tumour suppressor protein p53 and reactive oxygen species, but not redox activity, as critical elements in cytotoxicity. Mol Microbiol, 2003, 47: 549–559
19 Punj V, Das Gupta T K, Chakrabarty A M. Bacterial cupredoxin azurin and its interactions with the tumor suppressor protein p53. Biochem Biophys Res Commun, 2003, 312: 109–114
20 Apiyo D, Wittung S P. Unique complex between bacterial azurin and tumor suppressor protein p53. Biochem Biophys Res Commun, 2005, 332: 965–968
21 Yamada T, Hiraoka Y, Ikehata M, *et al.* Apoptosis or growth arrest: Modulation of tumor suppressor p53's specificity by bacterial redox protein azurin. Proc Natl Acad Sci USA, 2004, 101: 4770–4775
22 Hubbell W L, Cafiso D S, Altenbach C. Identifying conformational changes with site-directed spin labeling. Nat Struct Mol Biol, 2000, 7: 735–739
23 Fanucci G E, Cafiso D S. Recent advances and applications of site-directed spin labeling. Curr Opin Struct Biol, 2006, 16: 644–653
24 Hubbell W L, Gross A, Langen R, *et al.* Recent advances in site-directed spin labeling of proteins. Curr Opin Struct Biol, 1998, 8: 649–656
25 Colunbus L, Hubbell W L. A new spin on protein dynamics. Trends Biochem Sci, 2002, 27: 288–295
26 Hustedt E J, Beth A H. Nitroxide spin-spin interactions: applications to protein structure and dynamics. Annu Rev Biophys Biomol Struct, 1999, 28: 129–153
27 van de Kamp M, Hali F C, Rosato N, *et al.* Purification and characterization of a non-reconstitutable azurin, obtained by heterologous expression of *Pseudomonas aeruginosa azu* gene in *Escherichia coli*. Biochim Biophys Acta, 1990, 1019: 283–292
28 Bullock A N, Henckel J, DeDecker B S, *et al.* Thermodynamic stability of wild-type and mutant p53 core domain. Proc Natl Acad Sci USA, 1997, 94: 14338–14342
29 Bulaj G, Kortemme T, Goldenberg D P. Ionization-reactivity rela-

tionships for cysteine thiols in polypeptides. Biochemistry, 1998, 37: 8965–8972
30 Dunham T D, Farrens D L. Conformational changes in rhodopsin: movement of helix f detected by site-specific chemical labeling and fluorescence spectroscopy. J Biol Chem, 1999, 274: 1683–1690
31 Crane J M, Mao C, Lilly A A, *et al.* Mapping of the docking of Sec A onto the chaperone Sec B by site-directed spin labeling: insight into the mechanism of ligand transfer during protein export. J Mol Biol, 2005, 353: 295–307
32 Berliner L J. Spin Labeling: Theory and Applications. 2nd ed. New York: Academic Press, 1979
33 Lai C S, Froncisz W, Hopwood L E. An evaluation of paramagnetic broadening agents for spin probe studies of intact mammalian cells. Biophys J, 1987, 52: 625–628
34 Zhao B L, Li X J, He R G, *et al.* ESR studies on oxygen consumption during the respiratory burst of human polymorphonuclear leukocytes. Cell Biol Int, 1989, 13: 317–323
35 Rizzuti B, Sportelli L, Guzzi R. Evidence of reduced flexibility in disulfide bridge-depleted azurin: a molecular dynamics simulation study. Biophys Chem, 2001, 94: 107–120
36 Miller R. Simultaneous Statistical Inference. New York: Springer, 1981
37 Taranta M, Bizzarri A R, Cannistraro S. Probing the interaction between p53 and the bacterial protein azurin by single-molecule force spectroscopy. J Mol Recognit, 2008, 21: 63–70
38 De Grandis V, Bizzarri A R, Cannistraro S. Docking study and free energy simulation of the complex between DNA-binding domain and azurin. J Mol Recognit, 2007, 20: 215–226